532.55 : 532.517

Entrance Loss for Turbulent Flow without Swirl between Parallel Discs*

By Tatsuji KAWAGUCHI**

This paper is concerned with the investigation on the entrance loss which occurs in a radial turbulent flow between parallel discs. Because the theoretical determination of the entrance loss is almost impossible, the author has constituted an empirical equation by using nondimensional quantities — the space between the discs, the radius of rounded corner at entry boundary etc.— which have large influences on the entrance loss.

This equation will be usefull for the solution of practical problems.

1. Introduction

Radial flow of a fluid in a narrow gap between two parallel discs can take place in a radial diffuser, plate valve and seat, air micrometer and air bearing; and in such a case there are an inlet region near the entrance and a fully developed flow region in the downstream. The flow in the inlet region has a great influence upon the whole.

The theoretical study of the inlet region almost exclusively deals with laminar flow. For instance, the analytical solutions in which the inlet region is taken into consideration are Woolard's[1] and Hagiwara's[2], both of them using an approximate method of momentum integral. Ishizawa's[3][4] series solution of boundary layer equations include a separated region as well. These researches belong to the same category. But each of these theories presupposes that the thickness of the boundary layer is zero at the entry, and the fluid flows in along the wall, so that it is only to the case where the entrance form is ideal that the solution of this sort can be applied. The calculation of the boundary layer in the case of turbulent flow is so complicated that the condition that the fluid flows in along the wall at the entrance can not be satisfied in practice. Namely, the influence of the entrance form is large, so it is possible that this influence is exerted on the outlet also.

Though the study of the turbulent flow is very important, its study has scarcely been made hitherto, owing to the complication of such a flow. P.S. Moller[5] has been engaged in the study of the turbulent flow in parallel discs, but he has not dealt with the inlet region in detail.

The items concerned with the inlet region are the range of this region, the value of minimum pressure, the amount of hydraulic loss near the entrance, and the entrance form to influence upon inlet loss. With regard to this inlet loss there is only Nakayama's[6] study dealing with laminar flow.

In this paper are reported the results of the experimental study of above-mentioned items.

2. Notation

- h: gap of the discs $=2B$
- m: non-dimensional quantity of the gap $=B/r_1$
- P: total pressure
- p: static pressure
- Q: volume flow
- R: roundness of inlet corner
- R_e: Reynolds number based on the inlet mean velocity
- r: radius from the disc center
- r_b: value of r at the end of the inlet region
- U_c: local maximum velocity in the center of the gap
- u: time mean velocity in the radial direction
- $\bar{u}$: space mean velocity in the radial direction
- z: axial co-ordinate measured perpendicular to the disc wall
- τ_0: wall shear stress
- ν: kinematic viscosity of fluid
- ρ: density of fluid
- ξ: coefficient of the entrance losses for the turbulent flow

* Received 13th May, 1969.

** Assistant Professor, Nagoya Institute of Technology, Showa-ku, Nagoya.

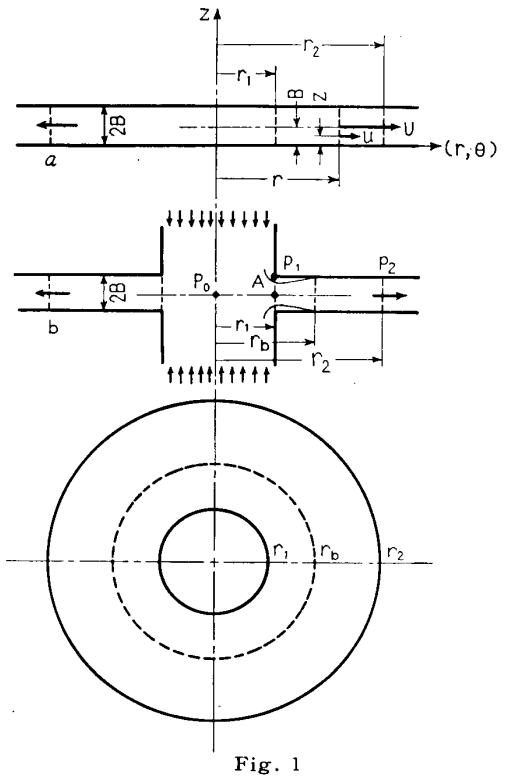

Fig. 1

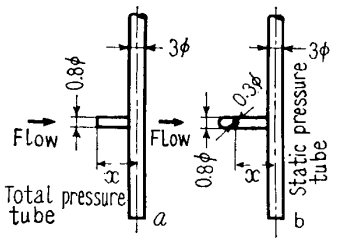

Subscripts

0 : at disc center
1 : at disc channel inlet
2 : at disc channel exit

3. A general consideration of turbulent radial flow

The case is considered where the fluid flows out radially between parallel discs as in Fig. 1 (a). For the case of axially symmetric fluid motion, we express the equations of motion in cylindrical polar co-ordinates r, θ, z. Taking shear stress at the wall as τ_0, the momentum equation for radial flow, considering an annular control volume, is[7]

$$\frac{1}{r}\frac{d}{dr}\left(r\int_0^B u^2 dz\right)=-\frac{\tau_0}{\rho}-\frac{1}{\rho}\frac{dp}{dr}\int_0^B dz \quad \cdots\cdots(1)$$

Assuming that the velocity profile is similar, the following equation is applicable to the turbulent flow

$$u/U=(z/\beta)^{1/7} \quad \cdots\cdots(2)$$

The equation for shear stress at the wall is

$$\tau_0=0.0225(\nu/BU)^{1/4} \quad \cdots\cdots(3)$$

Substituting these equations into Eq. (1) the following equation is obtained,

$$\frac{p-p_2}{1/2\rho\bar{u}_1^2}=-\frac{64}{63}r_1^2\left(\frac{1}{r^2}-\frac{1}{r_2^2}\right)+\frac{0.076}{mR_e^{1/4}}r_1^{3/4}\left(\frac{1}{r^{3/4}}-\frac{1}{r_2^{3/4}}\right) \quad \cdots\cdots(4)$$

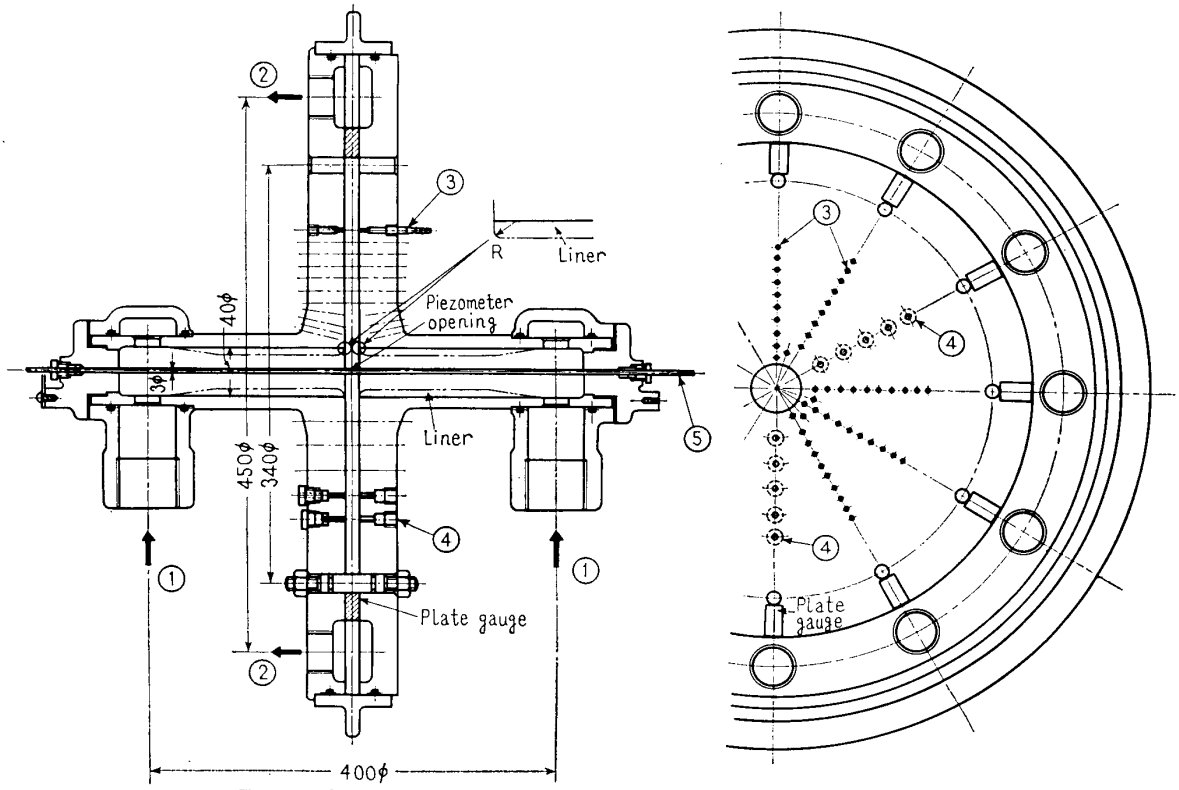

Fig. 2 Schematic diagram of test apparatus for parallel discs

In practice, as in the case of Fig. 1 (b), a fluid flows round an axis A at the corner of the entry, and the main flow runs in a quite different way from that of Fig. 1 (a). But this flow satisfies Eqs. (2) and (3) when it passes through the inlet region, and the pressure distribution satisfies Eq. (4). The first term in the right hand side of Eq. (4) shows the pressure rise due to inertia flow; and the second term shows the loss of pressure through wall friction. The difference between the total pressure at the center P_0 and total pressure at the exit P_2 consists of various losses at the entry and in the inlet region, and of the loss caused by wall friction. Wall shear stress in the inlet region does not satisfy Eq. (3), but for the convenience of calculation, assuming the existance of friction loss in the total region of the discs as shown in Eq. (4), and expressing the losses in the inlet region as $\xi(1/2)\rho\bar{u}_1^2$, it is given as

$$\xi\frac{1}{2}\rho\bar{u}_1^2=(P_0-P_2)-\frac{0.076}{mR_e^{1/4}}\left(1-\frac{r_1^{3/4}}{r_2^{3/4}}\right)\frac{1}{2}\rho\bar{u}_1^2$$

Taking the velocity distribution at r_2 as in Eq. (2) and putting $P_2=p_2+\frac{64}{63}(r_1/r_2)\frac{1}{2}\rho\bar{u}_1^2$, the following relation is obtained.

$$\frac{P_0-p_2}{(1/2)\rho\bar{u}_1^2}=\frac{64}{63}\left(\frac{r_1}{r_2}\right)^2+\frac{0.076}{mR_e^{1/4}}\left(1-\frac{r_1^{3/4}}{r_2^{3/4}}\right)+\xi \quad \cdots\cdots(5)$$

Where ξ is the coefficient of the inlet loss for turbulent flow. The factors that exert influence upon the value of ξ are the losses caused by the abnormal velocity distribution just before the entrance, contracted flow, separation, back flow on the wall surface. Supposing the inlet region to end at r_b, the flow from r_b to r_2 satisfies Eq. (4), and the factor that exerts influence upon ξ does not exist. Accordingly at the downstream from r_b, ξ takes a constant value.

4. Experimental apparatus and methods

The details of parallel discs used in the experiments are shown in Fig. 2. The water flows in from (1) and flows out in the direction of (2). The surfaces of discs are smoothly finished by lapping, and gap width between the discs is varied by spacer plates of different thicknesses (1, 2, 3, 5, 7 and 10 mm respectively). Tap (3) for the measurement of static pressure

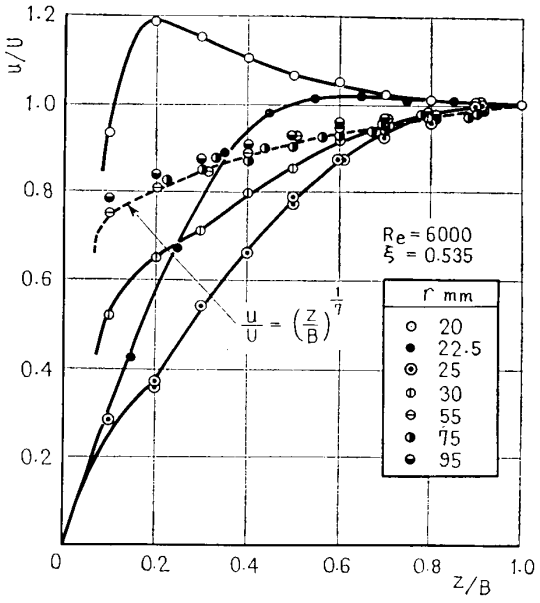

(b) Velocity distribution of $R=2$ mm, $h=10$ mm

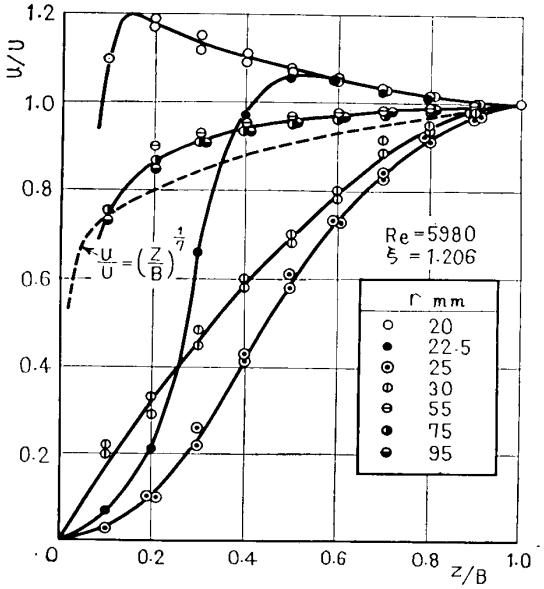

(a) Velocity distribution of $R=0$, $h=10$ mm

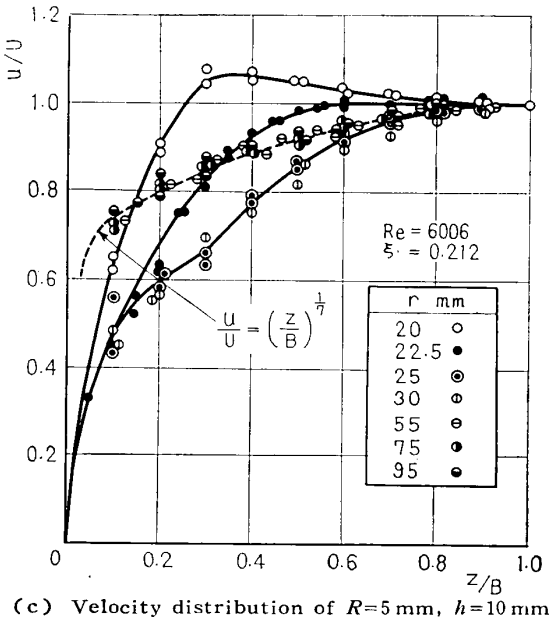

(c) Velocity distribution of $R=5$ mm, $h=10$ mm

Fig. 3

was bored at intervals of 5 mm along the radius, and the hole (4) for velocity measurement was bored at the intervals of 20 mm. The Pitot total pressure tube a and the static pressure tube b as shown in the figure were used. The distance of the pressure measuring orifice of the Pitot tube x is varied (20, 17.5, 15, 10 and 5 mm respectively). The total pressure at the center, P_0, is obtained from the piezometer opening of the tube (5). The roundness of the corner of the entrance R was varied by an inserted liner as shown in Fig. 2; and the values of R, are made 0, 0.3, 1, 2, and 5 mm. For the discs with the roundness R =0, 1, 2 and 5 mm respectively the ratio of radii $r_2/r_1=6$, and for the disc with $R=0.3$ mm, $r_2/r_1=0.784$.

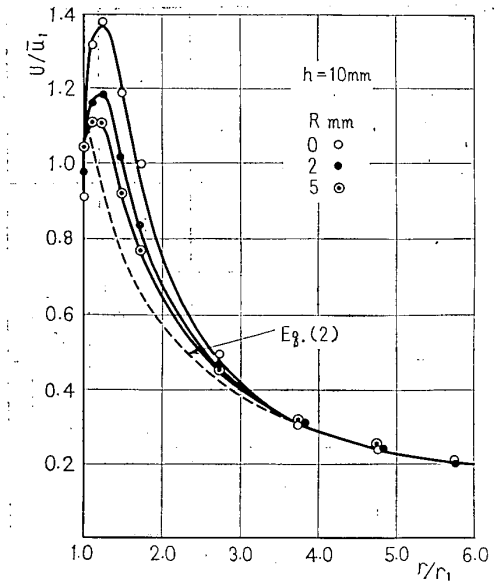

Fig. 4 Comparison between measured value of velocity in the center of gap $U/\bar{u}_1$, and calculated value of Eq. (2)

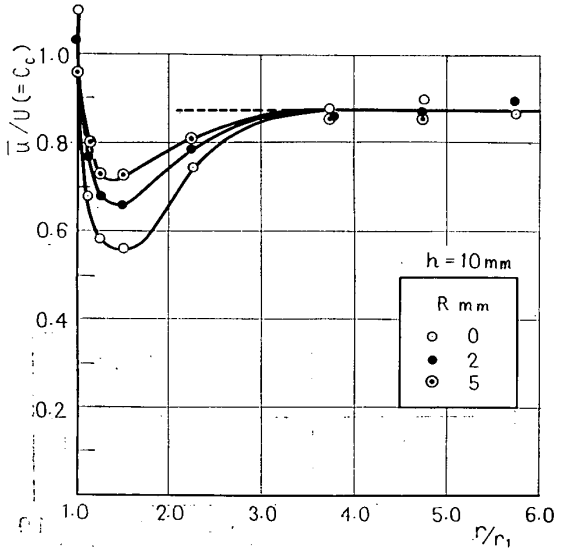

Fig. 5 Relation of $\bar{u}/U$ to r/r_1

5. Experimental results

5·1 On the velocity distribution and separation

The results of the velocity measurement at the gap are shown in Fig. 3. Here the discs

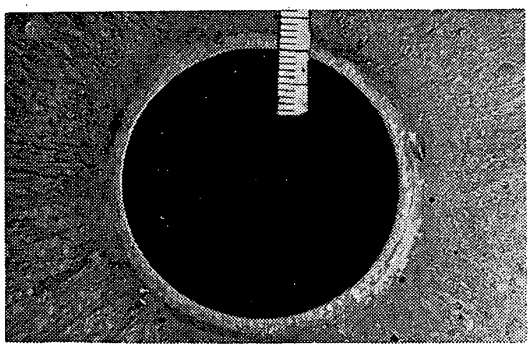

$R=0$, $h=1.0$ mm, $Re\fallingdotseq2\,000$, $\bar{u}_1=405.7$ cm/sec, $t=19.8$°C
(a)

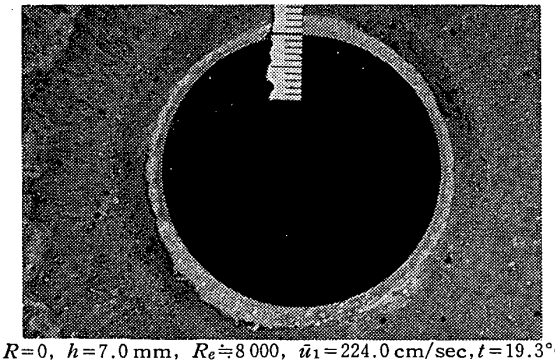

$R=0$, $h=7.0$ mm, $Re\fallingdotseq8\,000$, $\bar{u}_1=224.0$ cm/sec, $t=19.3$°C
(b)

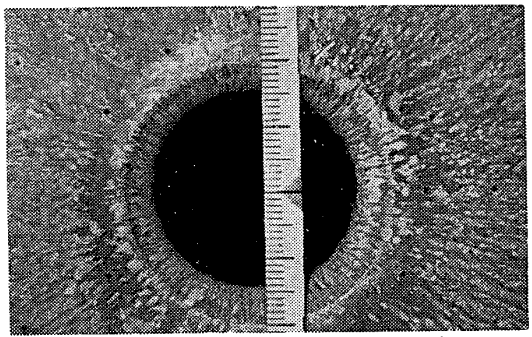

$R=5.0$ mm, $h=1.0$ mm, $Re\fallingdotseq2\,000$, $\bar{u}_1=396.8$ cm/sec, $t=20$°C
(c)

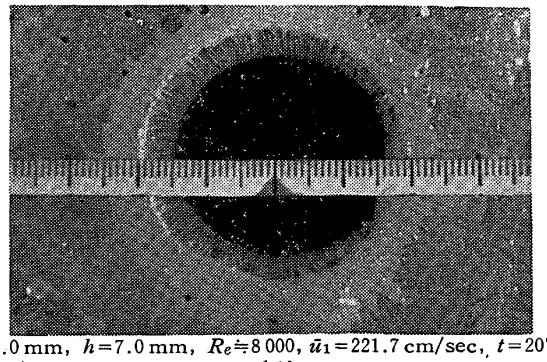

$R=5.0$ mm, $h=7.0$ mm, $Re\fallingdotseq8\,000$, $\bar{u}_1=221.7$ cm/sec, $t=20$°C
(d)

Fig. 6 Trace of flow near the entrance of discs

have in common the gap distance, 10 mm, and the inlet Reynolds number, $R_e=6\,000$. Figures 3 (a), (b) and (c) show the comparison of the velocity profiles with various inlet roundness. The velocity profile at the inlet of the channel ($r_1=20$ mm) shows a peculiar form, and the maximum velocity takes place near the wall, the velocity profile becoming concave towards the center. By decreasing the roundness of the inlet corner, the position of the maximum velocity shifts to the wall, and the concavity increases at the same time.

This phenomenon is caused by the influence of the flow turning around the corner of the entrance. As is shown in the velocity distribution at $r=22.5$ and 25 mm, the flow velocity near the wall retards rapidly within the distance of several mm, causing remarkable resistance or separation.

Moreover, when r is increased, the flow velocity rises again near the wall, and within the range of $r>55$ mm, the velocity distribution becomes almost similar.

In Fig. 4, the measured value of the velocity U at the center of the gap is compared with the value calculated by Eq. (2). The smaller is R, the larger becomes the measured value of U near the entrance, and the measured value coincides with the calculated value as r/r_1 increases.

Figure 5 shows the coefficient of contraction for varied shaped entry boundary when the width of gap is 10 mm. Now, assuming the width of vena contracta is B' and also the fluid flows though here with the uniform velocity U, the coefficient of contraction is calculated to be $C_c=B'/B=\bar{u}/U$. In Fig. 5 the minimum value of $\bar{u}/U$ is found to be 0.564 when $R=0$, and 0.660 when $R=2$ mm. These values agree with the contraction coefficient, 0.62 of an orifice. On the other hand, when $R=5$ mm, the coefficient becomes 0.728, and if the velocity distribution is assumed as Eq. (2), the ratio $\bar{u}/U$ is calculated to be 0.875. This value is shown by the dotted line, and at the downstream of the inlet region it coincides almost with measured value.

In order to make the flow phenomena clearer, Pb_3O_4 was dissolved in oil and spread on the disc surface to observe the separation growth. Plates (a) and (b), in Fig. 6 show the case in which $R=0$, and (c) and (d), show the case in which $R=5$ mm and in both cases, the discharge, gap-size and diameter at the entry are the same. The white ring-like parts appearing at the entrance are the separation region which occurs owing to the strong back flow as sketched in Fig. 7. On the other hand, in (c) and (d), such separation does not occur, and herein also the paint remains in a thin stratum, and separation can be discerned by the shade of colour. In the case of (c), as the flow velocity is high on this surface, small parts of thin stratun are seen to be dispersed.

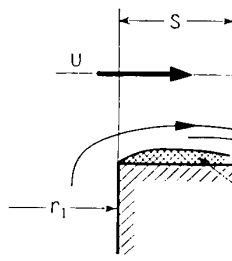

Fig. 7 Reverse flow on the wall near the entrance

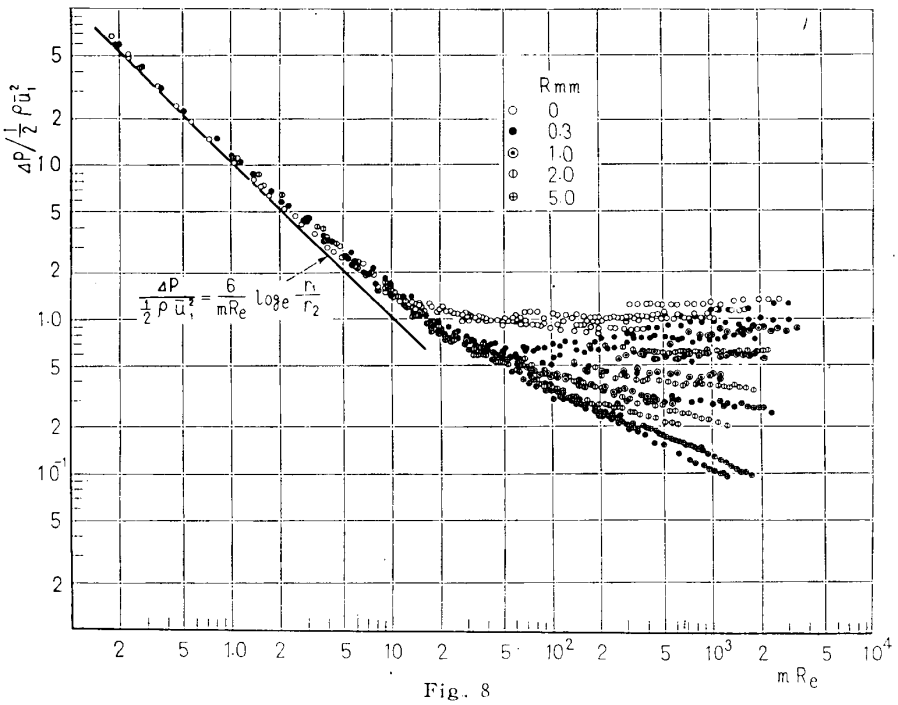

Fig. 8

5·2 The relation between Reynolds number and the pressure difference between entry and exit

The differential pressure Δp between P_0 and p_2, takes different values according to the

gap-size, the roundness of corner, discharge, etc. The value of $\Delta p/(1/2)\rho\bar{u}_1^2$ in the turbulent flow is represented by Eq. (5), and in the laminar flow is represented as follows[8],

$$\Delta p \Big/ \frac{1}{2}\rho\bar{u}_1^2 = \frac{54}{35}\left(\frac{r_1}{r_2}\right)^2 + \frac{6}{mR_e}\log_e\frac{r_2}{r_1} + \xi \quad \cdots\cdots(6)$$

These contain $mR_e^{1/4}$ and mR_e in the friction term respectively. The values of $\Delta p/(1/2)\rho\bar{u}_1^2$ against mR_e are plotted in Fig. 8. Using the same symbol points, the results with the gap sizes, 1, 2, 3, 5, 7 and 10 mm are shown to simplify the figure. When mR_e is below 1.0, the differential pressure Δp nearly coincides with the value calculated by Eq. (6). Accordingly within this range, the approximate calculations, with simplified inlet conditions, tried by many researchers hitherto are nearly cerrect. When mR_e= 1.0~10, Δp deviates from the calculated value, but the effect of the roundness of entry boundary R does not appear distinctly. When $mR_e=10$, points of $R=0$ branch off from the group of points distributed in a straight line. When mR_e =50, points of $R=0.3$ mm diverge in the same way. These phenomena show that the influence of the entry loss has begun to appear. According to these experimental results, it is concluded that the transition from laminar to turbulent flow first occurs near the entrance, and the turbulent state spreads outward in the downstream direction with increase of discharge, covering the total range of the discs at last. Figure 9 shows plots of $\Delta p/(1/2)\rho\bar{u}_1^2$ against R_e to clarify this critical Reynolds number. As the difference of the gap-size becomes distinct in this figure, the dimension of the gap has been written at the experimental points of $R=0$. It is the same with other Rs. In the case where $R=0$, the point branching off towards the turbulent flow line is $R_{ec}=200$ when the gap size is large; and with the decrease of the gap size, R_{ec} increases, and when the dimension of gap 1 mm, $R_{ec}=500$. From the comparison of the flow in the rectangular tube with the flow in the circular tube, the critical Reynolds number 500 in this experiment corresponds with 2000 of the circular tube[9][10]; but when the gap is large, owing to the contraction, etc. the transition occurs at a Reynolds number lower than that.

5·3 The pressure distribution for the turbulent flow and the radius r_b of the inlet region

In the case of $r_2/r_1=6$, if the Reynolds number at the entrance is over 3000, the flow is turbulent throughout the entire disc channel, and under this condition the pressure distribution may be calculated in accordance with Eq. (4). In practice, as there is a disturbunce near the entrance, the pressure distribution becomes different from that given by Eq. (4).

Figure 10 shows the comparison of the calculated value with the measured value. The measured pressure falls below the calculated value, but this is due to the contraction etc. Accordingly, as the flow region becomes more distant from the entrance, the measured value approaches the calculated value. When the minimum pressure measured at the entrance (the measured position, $r=25$ mm) is plotted in relation to R, it becomes as is shown in Fig. 11. The larger gap and the smaller R give the lower pressure.

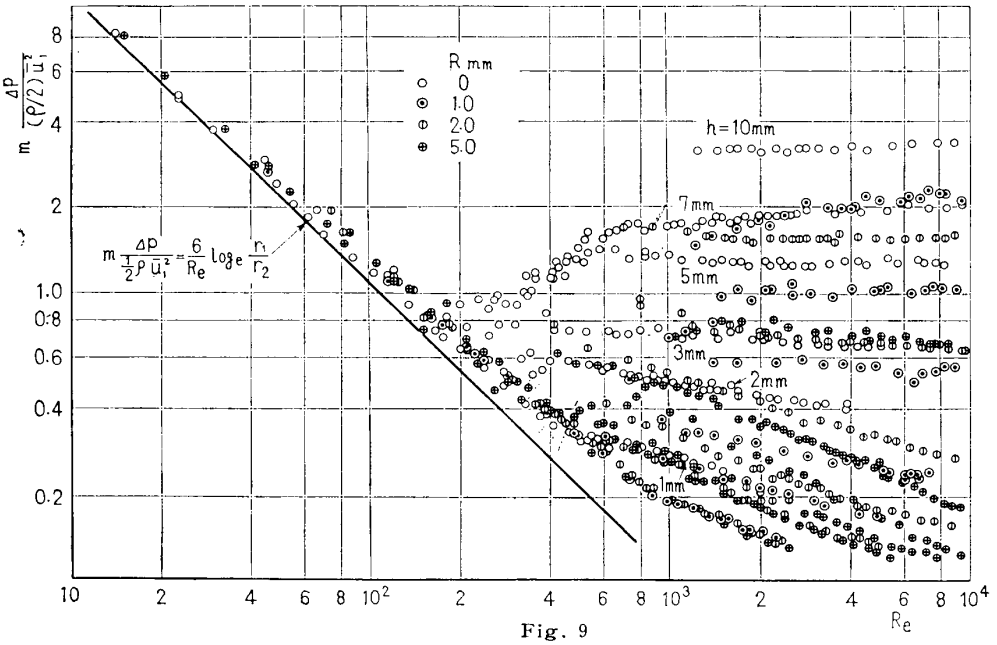

Fig. 9

Next, it is tried to decide the value of r_b from the measured result of the pressure distribution. Now, taking the total pressure at the center P_0 as a basis of the pressure, ξ is considered as a function of r in the same sense as in Eq. (5).

$$\xi(r)=\frac{P_0-p}{(1/2)\rho\bar{u}_1^2}-\frac{0.076}{mR_e^{1/4}}\times\left\{1-\left(\frac{r_1}{r_2}\right)^{3/4}\right\}-\frac{64}{63}\left(\frac{r_1}{r_2}\right)^2 \quad \cdots\cdots(7)$$

This ξ, which as one example is shown in Fig. 12-A, approarches gradually the constant ξ_0. Then taking the radius which has become 1.05 ξ_0, for convenience's sake, to be r_b, the value of r_b/r_1 can be found as a function of m and R. These are shown in Fig. 12-B. The ratio r_b/r_1 increases with the increase of m, and R.

5·4 The coefficient of entry loss in turbulent flow

In the case of $r_2>r_b$, ξ can be calculated from the experimental value, using Eq. (5). Figure 13 gives the relationship between values ξ and m for the various-shaped-entry boundary. When the radius R of the roundness becomes

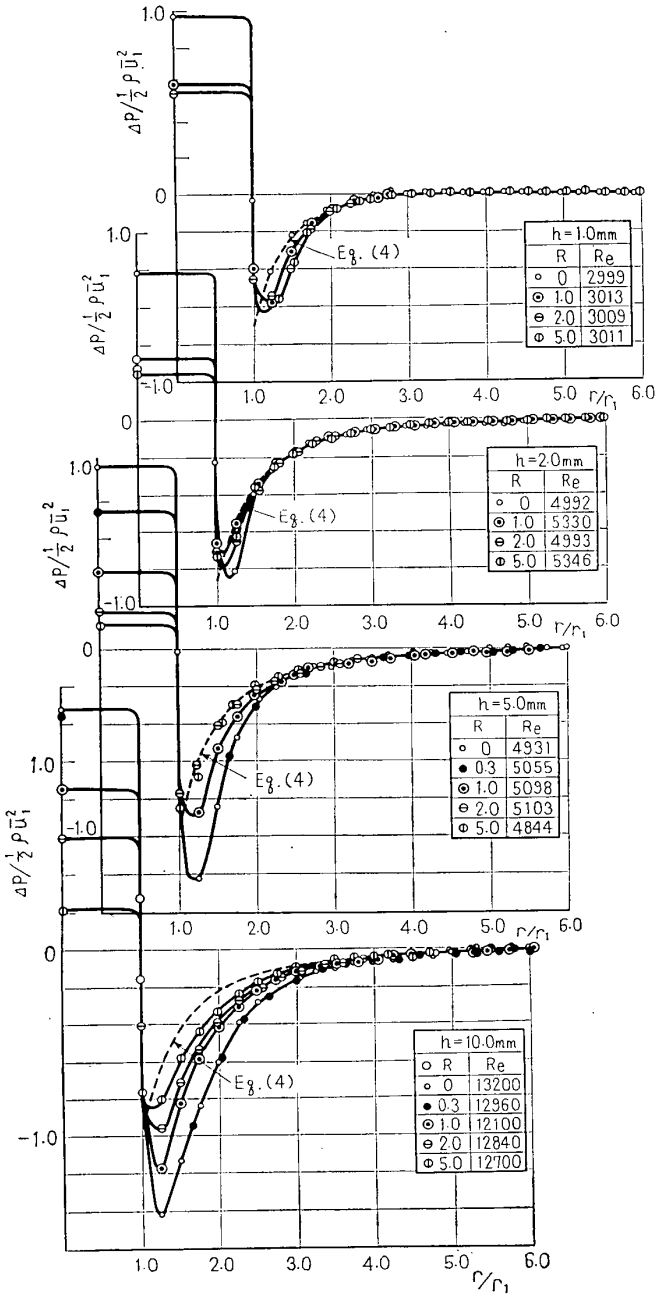

Fig. 10 Pressure distribution

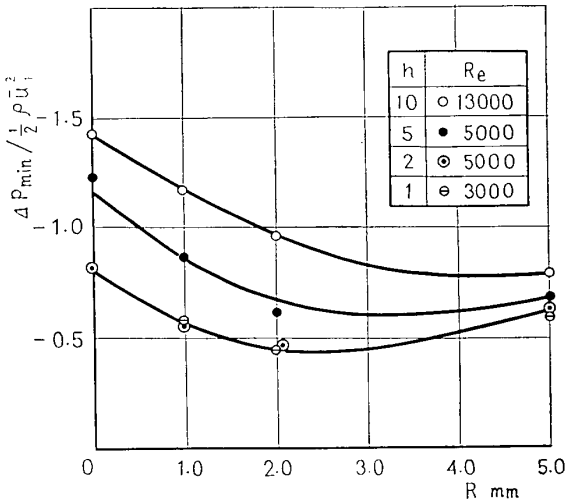

Fig. 11 Relation of minimum pressure to corner radius

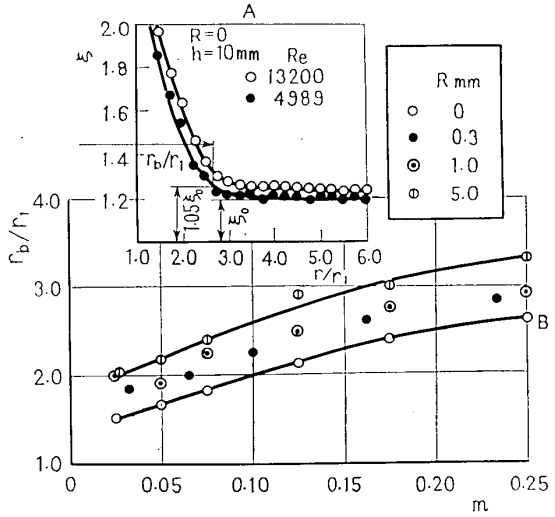

Fig. 12 Relation of r_b/r_1 to m

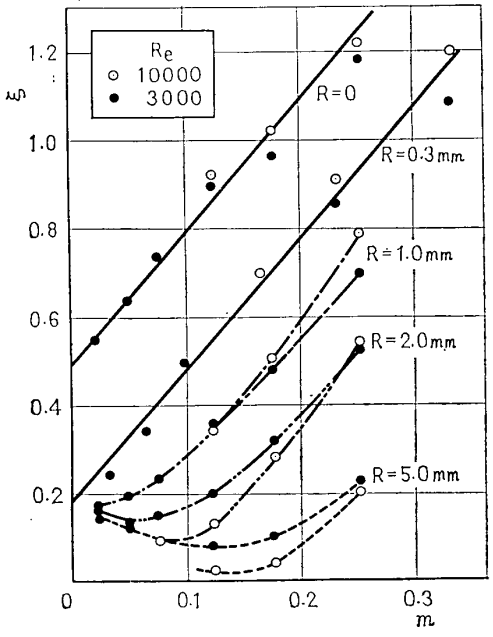

Fig. 13 Coefficient of entrance loss for turbulent flow ξ

smaller, ξ becomes a straight line of almost the same inclination as m. When R is large, and m becomes smaller, ξ deviates from the straight line and changes into concave shape, taking the minimum value at a certain value of m.

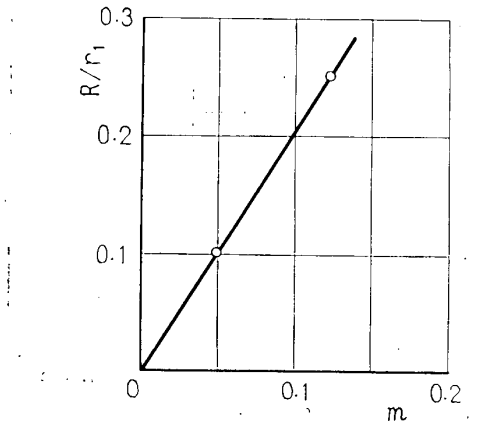

Fig. 14 Relation between optimum value of R/r_1 which makes ξ minimum and m

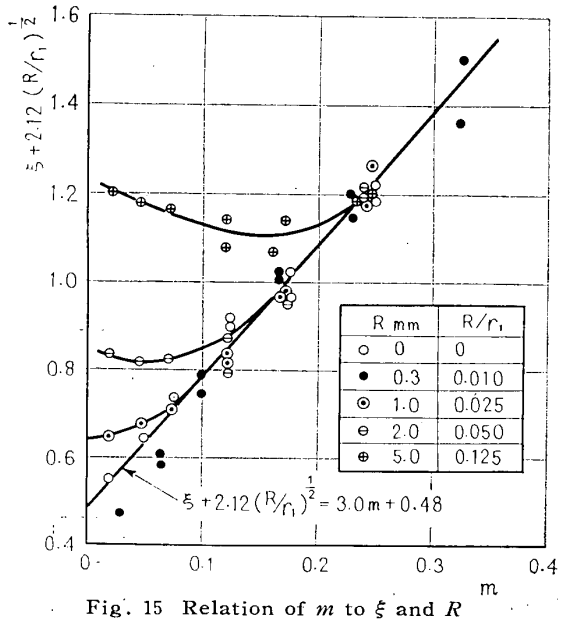

Fig. 15 Relation of m to ξ and R

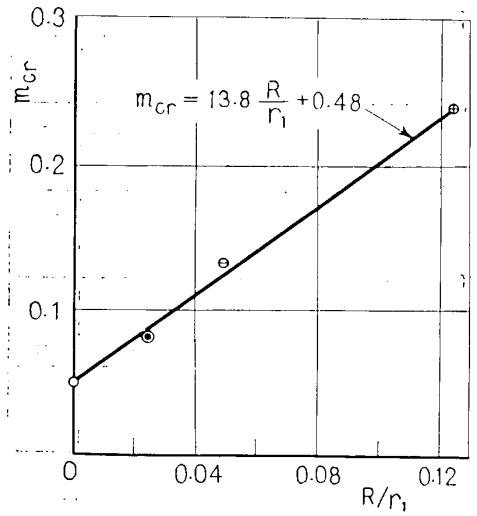

Fig. 16 Relation of R/r_1 to m_{cr}

The reason why ξ changes linearly is that the contraction and separation which are generated near the entrance grow larger with the increase of m. On the other hand, when R becomes larger, the contraction and separation are diminished, and the influence of m becomes smaller. But, in this case, the boundary layer is generated in the round parts of the corner. When the thickness δ of this boundary layer is larger than B, this becomes the inlet resistance at the entrance and increases the loss. In other words, as the gap $h=2B$ becomes smaller (m also becoming smaller), ξ increases. But if the gap becomes larger, though a small roundness may exist at the entry, the contraction and separation occur in the inlet region, and increase the value of ξ. Accordingly the optimum value of R which makes the value ξ minimum always exists in the gap of certain size. In this experiment, it is when $R=$ 2 and 5 mm that the minimum value of ξ appears. The relation between m and R at this point becomes a straight line passing through the origin as is shown in Fig. 14, and from this can be obtained the dimension of the gap and R. The empirical equation of ξ, can be expressed as

$$\xi=3.0m-2.12(R/r_1)^{1/2}+0.48 \quad \cdots\cdots(8)$$

By using the above equation, Fig. 13 can be plotted as one branched-out curve like Fig. 15. If the roundness exists at the corner, ξ branches off from this straight line corresponding to its size R. If the value m at the point branched off from the curve of ξ is expressed by m_{cr}, the relation between m_{cr} and R/r_1 becomes a straight line as shown in Fig. 16 and from this the following equation can be obtained.

$$m_{cr}=13.8(R/r_1)+0.48 \quad \cdots\cdots(9)$$

Namely, for a given value of R/r_1, m_{cr} is calculated by Eq. (9), and then comparing m_{cr} with m, if m is larger than m_{cr}, ξ becomes larger than this value.

6. Conclusions

On the entrance loss in the inlet region of the turbulent flow between parallel discs, the following have been clarified;

1. In the case where the flow is laminar, and Reynolds number is low, the effect of inlet region upon the total flow resistance can scarcely by discerned. Accordingly, it is possible to calculate the pressure difference at the entry and outlet only by consideration of the viscous term, neglecting the influence of entry boundary shape.

2. The difference between the pressure at the center and that at the outlet, changes suddenly when Reynolds number $B\bar{u}_1/\nu$ is 200～500. This is the transition from laminar to turbulent flow at entry.

3. As the gap increases and R decreases, the minimum pressure is generated near the entrance.

4. The coefficient of entry loss for turbulent flow depends remarkably on m and R, but the influence of R_e is small. There is the range in which ξ varies linearly to m, when a strong contraction and separation occur at the inlet. In the region in which ξ varies not linearly to m, there exists the value of m which gives minimum ξ. The reason why this phenomenon occurs can be explained by examining the boundary layer which is generated at the curved surface of the corner before the fluid flows into the parallel discs.

The author wishes to thank heartily Prof. Yoshimasa Furuya and Prof. Mitsukiyo Murakami of the Nagoya University for their consistent kind guidance, and Mr. Michihiko Kawaguchi for his cooperation in this experiment.

References

(1) Woolard, H.W., *Jour. Appl. Mech*, Vol. 24 (1957), p. 9.
(2) Hagiwara, T., *Bull. JSME*, Vol. 5, No. 20 (1962-9), p. 656.
(3) Ishizawa, S., *Bull. JSME*, Vol. 8, No. 31 (1965-8), p. 353.
(4) Ishizawa, S., *Bull. JSME*, Vol. 9, No. 33 (1966), p. 86.
(5) Moller, P.S., *Aeron. Quarterly*, Vol. 14 (1963), p. 163.
(6) Nakayama, Y., *Bull. JSME*, Vol. 7, No. 28 (1964-9), p. 698.
(7) Dorfman, L.A., *Hydrodynamic Resistance and the Heat Loss of Rotating Solids* (1st ed.), (1963), p. 55, Oliver and Boyd.
(8) Kawaguchi, T., *Bulletin of Nagoya Institute of Technology*, Vol. 19 (1967), p.173.
(9) Nikuradse, J., *Ingenieur Archiv.*, Bd.1 (1930), S. 306.
(10) Naumann, A., *Z. AMM.*, Sonderheft, Bd. 36 (1956), S. 25.